

## Micrometer and Sub Micrometer-Size Structures Fabricated by Direct Writing Using Femtosecond Light Pulses

E. Vanagas<sup>1,2</sup>, I. Kudryashov<sup>2</sup>, S. Juodkazis<sup>1,3</sup>, S. Matsuo<sup>3</sup>, H. Misawa<sup>4</sup>, R. Tomašiūnas<sup>1\*</sup>

<sup>1</sup>*Institute of Materials Science and Applied Research, Vilnius University, Saulėtekio 10, LT-2040 Vilnius, Lithuania*

<sup>2</sup>*Tokyo Instruments, Inc., 6-18-14 Nishikasai, Edogawa-ku, Tokyo 134-0088, Japan*

<sup>3</sup>*The University of Tokushima, 2-1 Minamijosanjima, Tokushima 770-8506, Japan*

<sup>4</sup>*Research Institute for Electronic Science, Hokkaido University, Sapporo 060-0812, Japan*

Received 23 September 2003; accepted 17 October 2003

In this report we present the results of the sub micrometer-size hillocks and bits recording on the surface and in the volume of dielectric materials using a direct femtosecond laser writing (DFLW) method. Lateral and axial dimensions of fabricated defects were measured ( $170 \pm 50$ ) and ( $440 \pm 100$ ) nm, respectively. 2D and 3D matrixes with the corresponding densities of 1 Gbit/cm<sup>2</sup> and 6 Tbit/cm<sup>3</sup> as well as waveguides were recorded using DFLW method.

**Keywords:** femtosecond fabrication, photomodification, nanostructuring, nanotechnology, waveguide, confocal, optical breakdown.

### INTRODUCTION

Laser microfabrication is one of the present actualities in the way to future technology development. Applied sciences constantly are moving to “nano-world”. Researchers in the fields of micro-electro-mechanical systems (MEMS) [1], life sciences [2], optical materials [3–5], etc. are making efforts to manipulate with dimensions in sub micrometer-scale. These structures are anticipated for diversity of possible applications as optoelectronic hybrid [6] and biochemical chips [7], waveguides [8], high-capacity optical memory devices [9], photonic crystals (PhC) [5], micromechanical systems [10], etc. To create structures of ultimately small size different techniques are implemented: ultra-violet lithography [11], electron, ion beam lithographies [12] and machining [13], near field lithography [14] and machining [15], nano-second laser writing [16, 17], positioning of single atoms with scanning tunneling microscope [18], etc.

Material treatment with femtosecond light pulses have exceptional advantages to fabricate micro-, nano-scale structures and are widely discussed in the past decade [19–24]. The key point of the process is the light pulse energy concentration in time and space. The intensities up to exa-watt ( $10^{18}$ ) per square centimeter can be achieved, which is far beyond the maximal threshold of laser ablation and three-dimensional recording in transparent dielectrics at  $10^{13} - 10^{14}$  W/cm<sup>2</sup>. The energy density is high enough to induce multi-photon transition of electron to conduction band in wide-band-gap high optical quality dielectrics. Light induced optical breakdown (LIOB) is developing as a sequence of multi-photon absorption with ensuing avalanche. The standard bell-shaped intensity profile of the pulse allows to localize the LIOB in space with practically any desired resolution with high precision. Ultra-short excitation is followed by electron-ion plasma generation and phase explosion or field-induced disintegration of

surface in the field of departing electrons. These are driving mechanisms of material ablation [25] from irradiated area. The field-induced disintegration is shorter than the time necessary to absorb the energy by lattice of the material and allow to achieve material removal from surface without a considerable thermal load, which cause cracking. These factors results into minimum material heating and negligible heat affected zone.

The method of DFLW could become a less expensive and productive for fabrication of ultra-small structures as compared to the usual photolithography and solid state technologies. Here we present the results on fabrication of sub micrometer-sized structures on and inside the dielectrics materials.

### EXPERIMENTAL

Experimental setup is based on Hurricane femtosecond laser (Spectra Physics) and the micromachining system (Tokyo Instruments, Inc.). Micromachining unit includes: optics, electronics and software (Tokyo Instruments, Inc.), a modified up-right type microscope (Olympus MX40), and piezostage (Polytec PI, Inc.). The setup and software allow to control the size of the focused beam spot on the sample, light polarization, intensity, number of pulses per point of irradiation, and the pattern via the computer-aided software.

Femtosecond pulses (wavelength  $\lambda_f = 800$  nm, duration 120 fs, repetition rate 1 kHz, beam quality factor  $M^2 < 1.5$ , and diameter  $d_f = 6$  mm) from a Hurricane output are directed through the micromachining unit, where polarization and intensity are attuned. Modified side port from Olympus is used to set femtosecond beam on the optical axis of the microscope. High magnification (100×) lenses were used for the fabrication experiments: a dry objective lens with  $NA = 0.95$  and an oil immersion one with  $NA = 1.40$  (Olympus). Pulse duration on the sample was evaluated to be about 180 fs, since the dispersion after approximately total 60 mm of glass in the system.

\*Corresponding author. Tel.: + 370-5-2698725.; fax: + 370-5-2698690.  
E-mail address: rolandas.tomasiunas@ff.vu.lt (R. Tomašiūnas)

The samples used in the experiments were borosilicate cover glass and crystalline quartz. Typically we obtained focal spots with a sub micrometer-diameter. The focusing of Gaussian beam for the employed experimental conditions corresponded to a diameter spot (waist diameter at FWHM)  $D = K \cdot \lambda_f \cdot M^2 / 2 \cdot NA$  [26], calculated for truncation ratio  $T = d_f / d_{lens}$  by objective lens with aperture  $d_{lens}$ . Parameter  $K$  is the beam truncation factor at FWHM;  $\lambda_f$  is the fs laser wavelength and  $M^2 = 1.5$  is the Hurricane beam quality factor. The waist length could be expressed as a doubled Rayleigh length  $L = 2z_R = 2\pi \cdot n_f \cdot \omega_0^2 \cdot M^2 / \lambda_f$ , where  $2\omega_0 = 1.27 \cdot \lambda_f \cdot f / d_f$  is diffraction limited waist diameter,  $f$  is the lens focal length. Additional beam quality factor relevant to the beam truncation could be calculated according to ref [26] as  $M_{Tr}^2 = d_{Tr} / 2\omega_0$ . Here,  $d_{Tr} = K_e \cdot \lambda \cdot f / d_{lens}$  is the truncated Gaussian beam waist diameter at the focus and  $K_e$  is the beam truncation factor, both at  $1/e^2$  intensity. Refractive index for  $\lambda_f = 800$  nm we approximately consider  $n_f = 1.47$  for the borosilicate cover glass and  $n_f = 1.542$  for the crystalline quartz. Actually, quartz is a double-refraction material and  $n_o = 1.538$ ,  $n_e = 1.547$ . These expressions were applied to calculate the beam waist diameter and doubled Rayleigh length:  $D = 0.68$ ,  $L = 0.65$  and  $D = 0.48$ ,  $L = 0.69$   $\mu\text{m}$ , respectively, for the surface and in-volume focusing cases.

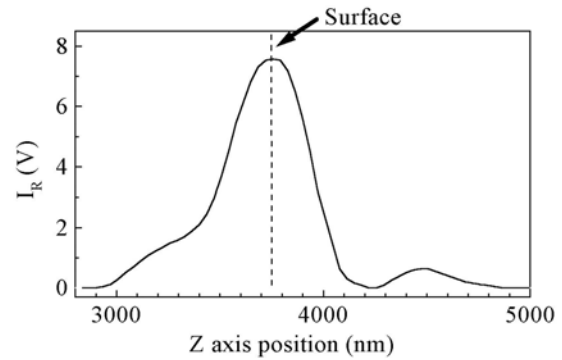
The sample was usually fixed on a three-axis piezostage and a chosen pattern was fabricated on or in the sample. A recording irradiation was positioned precisely on or below the surface of the sample by using a confocal laser microscope unit of the micromachining system. An auxiliary He-Ne laser ( $\lambda = 543.5$  nm) beam focus was tuned to overlap with the focus of the recording fs pulse. This confocal scheme, hereafter called the autofocus, tracked the reflection from the sample's surface and allowed the axial position of the surface to be controlled with a precision of 10 nm (root-mean-square value). This made it possible to track and compensate for the surface curvature during scanning. Such high-precision surface tracking was indeed necessary in order to keep the focus of the fs pulses on the surface in some experiments for the smallest feature size and for uniform photomodification/nano-structuring. Figure 1 shows a typical signal of He-Ne laser light reflection by the sample surface detected with a confocal laser microscope when the focus was axially translated. This confocal method allows positioning with high accuracy. The center-of-mass calculation of the area below curve  $I_R = f(z)$  enables repeatability of positioning to be kept within 10 nm (rms).

2D and 3D matrixes were recorded on the surface and inside the dielectrics aiming at the smallest size. Also, a waveguide recording is demonstrated.

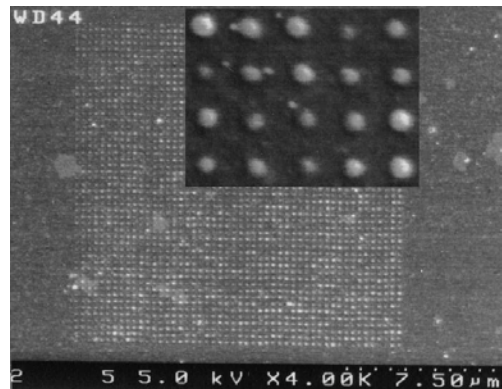
## RESULTS AND DISCUSSION

Figure 2 shows SEM images of a square pattern ( $15 \times 15$ )  $\mu\text{m}^2$  recorded with 5 nJ pulses on the surface of the cover glass. The lateral separation between irradiation

sites was 0.3  $\mu\text{m}$ . The lateral cross section of the hillocks was 115 – 155 nm for an approximately 15 nm Au layer. AFM measurements were carried out in order to prove that the bright sites in the SEM images were protuberant. We confirmed that the brighter regions observed in SEM were indeed the ablation-formed hillocks of 40 – 70 nm high. This kind of photomodification of a glass surface can be called nanostructuring, since both the lateral size and the height are less than 100 nm, which is considered the “size threshold” of nanotechnology.



**Fig. 1.** Intensity  $I_R$  detected by confocal laser microscope, when focus of He-Ne laser beam is axially translated. Maximum intensity corresponds to the focus point on the sample surface



**Fig. 2.** SEM image of the matrix recorded on the surface of the cover glass. Pitch size is 300 nm. Inset shows enlarged area of the matrix

The pulse energy range at which the formation of hillocks was observed was about 5 nJ at our focusing conditions (corresponding to 7.6 TW/cm<sup>2</sup> irradiance when 0.68  $\mu\text{m}$  FWHM spot size was considered). It is noteworthy that this kind of surface modification is inherently debris free. For the higher pulse energies, crater-like ablation sites, typically, include a considerable debris deposition. The hillock formation at a damage site is consistent with the mechanism of the field-induced disintegration of surface in the field of departing electrons. This mechanism has already been confirmed for crystalline dielectrics such as Al<sub>2</sub>O<sub>3</sub>, NaCl, and BaF<sub>2</sub> [27 – 29], where high energy ions were detected after the departure of electrons.

The formation of hillocks without obvious melting and crater pitting proves that material starts to leave the surface before melting or vaporizing occurs, i.e., the absorbed

energy is deposited to the electrons which had not enough time to transfer it to the ions. The lateral dimensions of the damage site were 4–6 times smaller than the calculated spot diameter on the sample at our focusing conditions. This is consistent with a multiphoton characteristic of the damage-inducing mechanism [30]. For this reason, the stability of the laser pulse energy and the precision of the focal spot positioning are both key to nanostructuring with a 100 nm feature size on a glass surface (the estimated density of bits corresponds to approximately 1 Gbits/cm<sup>2</sup>).

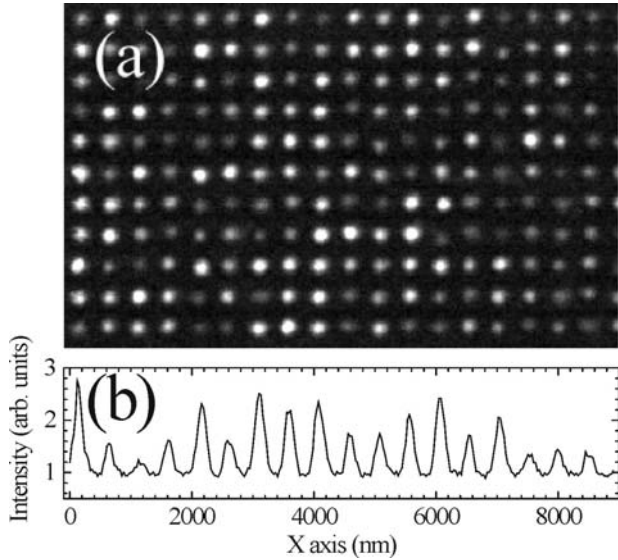


**Fig. 3.** The confocal scanning image of the fabricated matrix at the x-y cross-section plane (a); and a scattered light intensity distribution for one of the x-direction rows of the bits (b). Defects sizes at FWHM were evaluated to be (170 ± 50) nm

The other relevant question is, what is the smallest inbulk damage, i.e., a voxel that can be recorded in glass? Recently, we have shown that damage smaller than 200 nm can be recorded in silica [31].

Recording in this experiment was done by a single pulse of 800 nm wavelength using an oil-immersion objective lens with  $NA = 1.4$ . Figures 3 and 4 represent the matrix of  $20 \times 20 \times 5$  points (for x-y-z axes) written in the volume of the quartz plate with lateral and axial steps equal 0.5  $\mu\text{m}$  and 0.67  $\mu\text{m}$ , respectively. First layer is 5  $\mu\text{m}$  below surface; pulse energy is  $E_p = 10$  nJ that corresponds to the density of power  $I_p = 31 \times 10^{12}$  W/cm<sup>2</sup> for the focusing conditions when  $D = 0.48$   $\mu\text{m}$ .

Scanning data of the fabricated pattern inside the volume is obtained with *Nanofinder*<sup>®</sup> system (Tokyo Instruments, Inc.). This is a confocal laser microscope with spectrometer. The measurements were performed in the mode of laser scattered light detection (argon cw laser,  $\lambda_{CW} = 488$  nm). The resolution for the lateral and axial dimensions at FWHM calculated according [32]:

$$\delta r = 0.51 \frac{\lambda_{CW}}{NA} \quad \text{and} \quad \delta z = \frac{0.88 \cdot \lambda_{CW}}{\left( n_{CW} - \sqrt{n_{CW}^2 - NA^2} \right)}, \quad \text{where}$$

$NA = 1.4$  is objective lens numerical aperture;  $n_{CW} = 1.553$  is refractive index of crystal quartz for  $\lambda_{CW} = 488$  nm. The lateral and axial resolution values correspond to 178 nm, and 487 nm, respectively.

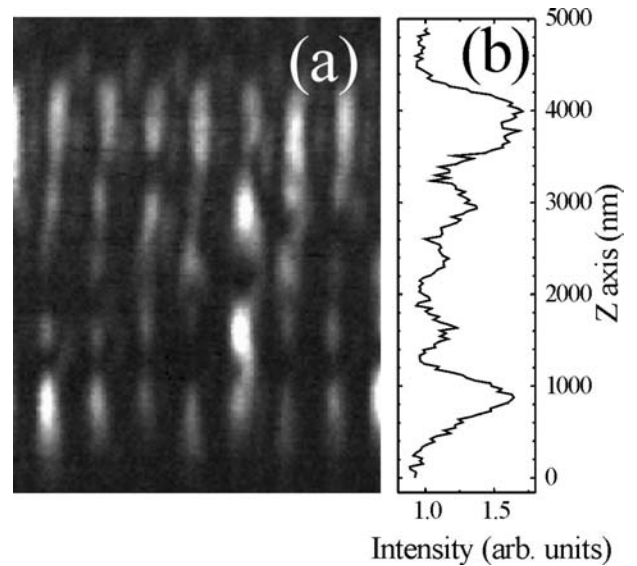


**Fig. 4.** The image of confocal scanning of fabricated matrix at the x-z plane cross-section (a); and the scattered light intensity distribution for one of z-direction columns of the bits (b). Defects sizes at FWHM were evaluated to be (440 ± 100) nm

The scanned image (Figure 3 (a)) shows x-y plane cross-section of the matrix directly written inside the volume of quartz with femtosecond laser pulses. The scanned signal intensity distribution of the bits row for x direction is shown in Figure 3 (b), where obtained widths vary (170 ± 50) nm at FWHM. Fig. 4 (a) shows part of the matrix x-z plane cross-sectional scan, where the signal intensity distribution for the vertical column of bits is shown in Fig. 4 (b). Here, the obtained widths values of bits are (440 ± 100) nm at FWHM. The obtained lateral and axial dimensions, in general, coincide with the resolution of *Nanofinder*<sup>®</sup> system ( $\delta r = 178$  nm,  $\delta z = 487$  nm). We suppose that the bit sizes are equal or below system resolution numbers, and the obtained values can be asserted as the upper limit for the bits dimensions. The density of the fabricated 3D structure is calculated to be 6 Tbits/cm<sup>3</sup>. We assert that this method capable to produce hundred-nanometer size defects in the volume that allows to obtain a higher than 100 Tbits/cm<sup>3</sup> density.

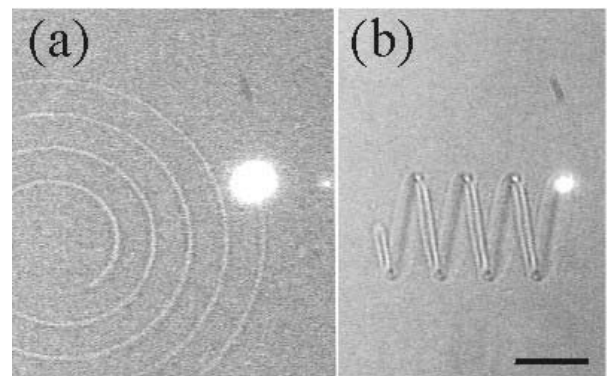


**Fig. 5.** Waveguide writing process: structure's top point is at 10  $\mu\text{m}$  below the glass surface. In situ images of recording of the vertical helix with an increasing radius (a) and horizontal helix (b). Scale bar 10  $\mu\text{m}$

The fabrication of waveguides is presented as an application example of the DFLW method. The structures

fabricated inside borosilicate glass are shown in Fig. 5. The permanent shooting at the pulse repetition rate of 1 KHz was implemented with the stage moving at constant speed while keeping the focal point on the trajectory of helix was employed to record the potentially waveguiding structures. The width of channel of modified glass was approximately 1  $\mu\text{m}$ . This example shows the possibilities of DFLW method for the 3D recording of complex freely positioned patterns applicable for an optical chips, waveguides, photonic crystals, and optical memory.

## CONCLUSIONS

The sizes of the hillocks and the bits, fabricated by direct femtosecond laser writing method were in the range of 100–200 nm in both cases: surface and volume fabrication. These small feature sizes are prospective for the high density and high precision structuring and fabrication using this method. Anticipated densities for the 2D and 3D bit patterns are higher than 1 Gbits/cm<sup>2</sup> and 100 Tbits/cm<sup>3</sup>, respectively. Fabrication precision is expected to be in the range of 100 nm making it interesting for the nanotechnology applications.

## REFERENCES

1. Maruo, S., Kawata, S. Two-Photon-Absorbed Near Infrared Photopolymerization for Three-Dimensional Micro-fabrication *Journal of Microelectromechanical Systems* 7 1998: pp. 411–415.
2. Nishimura, N., Schaffer, C. B., Li, E. H., Mazur, E. Tissue Ablation with 100-fs and 200-ps Laser Pulses *Proc. of the 20th Annual International Conference of the IEEE Engineering in Medicine and Biology Society* 20 (4) 1998: pp. 1703-1706.
3. Glezer, E. N., Mazur, E. Ultrafast-Laser Driven Micro-Explosions in Transparent Materials *Appl. Phys. Lett.* 71 1997: pp. 882–884.
4. Lenzner, M. Femtosecond Laser-Induced Damage of Dielectrics *International Journal of Modern Physics B* 13 1999: pp. 1559–1579.
5. Mizeikis, V., Juodkazis, S., Marcinkevicius, A., Matsuo, S., Misawa, H. Tailoring and Characterization of Photonic Crystals *J. of Photochemistry and Photobiology C: Photochemistry Reviews* 2 2001: pp. 35–69.
6. Leong, K. H., Said, A. A., Maynard, R. L. Femtosecond Micromachining Applications for Electro-Optic Components *Proc. of Electronic Components and Technology Conference (ECTC), Orlando, FL* 2001: pp. 210–214.
7. Ikuta, K., Maruo, S., Fujisawa, T., Yamada, A. Micro Concentrator with Opto-Sense Micro Reactor for Biochemical IC Chip Family - 3D Composite Structure and Experimental Verification *Proc. of 12th IEEE International Conference on Micro Electro Mechanical Systems (MEMS'99), Orlando, FL* 1999: pp. 376–381.
8. Schaffer, C. B., Brodeur, A., Garcia, J. F., Mazur, E. Micromachining Bulk Glass Using Femtosecond Laser Pulses with Nanojoule Energy *Opt. Lett.* 26 2001: pp. 93–95.
9. Watanabe, M., Sun, H., Juodkazis, S., Takahashi, T., Matsuo, S., Suzuki, Y., Nishii, J., Misawa, H. Three-Dimensional Optical Data Storage in Vitreous Silica *Jpn. J. Appl. Phys.* 37 1998: pp. L1527–L1530.
10. Kawata, S., Sun, H - B., Tanaka, T., Takada, K. Finer Features for Functional Microdevices *Nature (London)* 412 2001: pp. 697–698.
11. Driessen, F., Paul van Adrichem, Philipsen, V., Jonckheere, R., Liu, H - Y, Karklin, L. Aerial Image Simulations of Soft Defects in 193 nm Lithography for 100- and 70 nm Nodes *Proc of SPIE* 4691 2002: 127 p.
12. Juodkazis, S., Yamaguchi, A., Ishii, H., Matsuo, S., Takagi, H., Misawa, H. Photo-Electrochemical Deposition of Platinum on TiO<sub>2</sub> With Resolution of Tens-of-nm by Using a Mask Elaborated with Electron-Beam Lithography *Jpn. J. Appl. Phys.* 40 2001: pp. 4246–4251.
13. Gierak, J., Maily, D., Faini, G., Pelouard, J. L., Denk, P., Pardo, F., Marzin, J. Y., Septier, A., Schmid, G., Ferre, J., Hydman, R., Chappert, C., Flicstein, J., Gayral, B., Gerard, J. M. Nano-Fabrication with Focused Ion Beams *Microelectronic Engineering* 57–58 2001: pp. 865–875.
14. Ono, T., Esashi, M. Subwavelength Pattern Transfer by Near-Field Photolithography *Jpn. J. Appl. Phys.* 7 1998: pp. 6745–6749.
15. Scumacher, H. W., Keyser, U. F., Zeitler, U., Haug, R. J. Nanomachining of Mesoscopic Electronic Devices Using an Atomic Force Microscope *Appl. Phys. Lett.* 75 1999: pp. 1107–1109.
16. Ghantasala, M. K., Hayes, J. P., Harvey, E. C., Sood, D. K. Patterning, Electroplating and Removal of SU-8 Moulds by Excimer Laser Micromachining *J. Micromech. Microeng.* 11 2001: pp. 133–139.
17. Qin, S - J., Li, W. J. Micromachining of Complex Channel Systems in 3D Quartz Substrates Using Q-switched Nd:YAG laser *Appl. Phys. A* 74 2002: pp. 773–777.
18. Eigler, D. M., Schweizer, E. K. Positioning Single Atoms with a Scanning Tunneling Microscope *Nature (London)* 344 1990: pp. 524–526.
19. Pronko, P. P., Dutta, S. K., Squier, J., Rudd, J. V., Du, D., Mourou, G. Machining of Sub-Micron Holes Using Femtosecond Laser at 800 nm *Opt. Commun.* 114 1995: pp. 106–110.
20. Momma, C., Chichkov, B. N., Nolte, S., F. von Alvensleben, Tünnermann, A., Welling, H., Welleghausen, B. Short-Pulse Laser Ablation of Solid Targets *Opt. Commun.* 129 1996: pp. 134–142.
21. Perry, M. D., Stuart, B. C., Banks, P. S., Feit, M. D., Yanovsky, V., Rubenchik, A. M. Ultrashort-Pulse Laser Machining of Dielectric Materials *J. Appl. Phys.* 85 1999: pp. 6803–6810.
22. Korte, F., Adams, S., Egbert, A., Fallnich, C., Ostendorf, A., Nolte, S., Will, M., Ruske, J - P., Chichkov, B. N., Tünnermann, A. Sub-Diffraction Limited Structuring of Solid Targets with Femtosecond Laser Pulses *Optics Express* 7 2000: pp. 41–49.
23. Miwa, M., Juodkazis, S., Kawakami, T., Matsuo, S., Misawa, H. Femtosecond Two-Photon Stereo-Lithography *Appl. Phys. A* 73 2001: pp. 561–566.
24. Lenzner, M., Kruger, J., Sartania, S., Cheng, Z., Spielmann, Ch., Mourou, G., Kautek, W., Krausz, F. Femtosecond Optical Breakdown in Dielectrics *Phys. Rev. Lett.* 80 1998: pp. 4076–4079.
25. D. von der Linde, Sokolowski - Tinten, K. The Physical Mechanisms of Short-Pulse Laser Ablation *Appl. Surf. Sci.* 154–155 2000: pp. 1–10.

26. **Belland, P., Crenn, J.** Changes in the Characteristics of a Gaussian Beam Weakly Diffracted by a Circular Aperture *App. Opt.* 21 1982: pp. 522 – 527.
27. **Henyk, M., Wolframm, D., Reif, J.** Ultra Short Laser Pulse Induced Charged Particle Emission from Wide Bandgap Crystals *Appl. Surf. Sci.* 168 2000: pp. 263 – 266.
28. **Henyk, M., Mitzner, R., Wolframm, D., Reif, J.** Laser-Induced Ion Emission from Dielectrics *Appl. Surf. Sci.* 154 – 155 2000: pp. 249 – 255.
29. **Henyk, M., Costache, F., Reif, J.** Femtosecond Laser Ablation from Sodium Chloride and Barium Fluoride *Appl. Surf. Sci.* 186 2002: pp. 381 – 384.
30. **Schaffer, C. B., Brodeur, A., Mazur, E.** Laser-Induced Breakdown and Damage in Bulk Transparent Materials Induced by Tightly Focused Femtosecond Laser Pulses *Meas. Sci. Technol.* 12 2001: pp. 1784 – 1794.
31. **Juodkasis, S., Kondo, T., Mizeikis, V., Matsuo, S., Misawa, H., Vanagas, E., Kudryashov, I.** Microfabrication of Three-Dimensional Structures in Polymer and Glass by Femtosecond Pulses in *Proceedings of the Bilateral Conference on Optoelectronics and Magnetic Materials* Taipei, Republic of China (2002) (preprint available from arXiv:physics/0205025 v1 9 May 2002).

DOI: 10.5755/j02.ms.26730